

Materials Highlights

ISSN (Online): 2666-4933

ISSN (Print): N/A

Journal Home: <https://www.athena-publishing.com/journals/mahig>



Article Title

PVP-Induced Synthesis of Silica Nanoparticles With Tailored Size for pH-Controlled Drug Release

Authors

Wei Yang, Zheng Yang

Corresponding Author

Zheng Yang – zhengyang@fynu.edu.cn

Cite This Article As

W. Yang, Z. Yang. PVP-Induced Synthesis of Silica Nanoparticles With Tailored Size for pH-Controlled Drug Release. Materials Highlights, Vol. 2(3), pp. 52-57, 2021.

Link to This Article (DOI)

<https://doi.org/10.2991/mathi.k.210414.001>

Published on Athena Publishing Platform

31 January 2022

Research Article

PVP-Induced Synthesis of Silica Nanoparticles with Tailored Size for pH-Controlled Drug Release

Wei Yang¹, Zheng Yang^{2,*}

¹Institutes of Physical Science and Information Technology, Anhui University, Hefei 230601, P. R. China

²School of Chemistry and Materials Engineering, Fuyang Normal University, Fuyang 236037, P. R. China

ARTICLE INFO

Article History

Received 08 December 2020

Accepted 09 April 2021

Keywords

PVP-induced synthesis
SiO₂ nanoparticles
drug delivery
pH-controlled drug release
cancer treatment

ABSTRACT

Traditional cancer therapy faces the main fail due to the effect of drug burst release, hindering the long-term therapeutic efficacy. SiO₂ nano systems possess high-capacity and pH-controlled release for anti-cancer drug, improving the curative efficacy in cancer treatment. Thus, we designed a novel method to construct Silica Nanoparticles (SiO₂ NPs) with diameters of ca. 150 nm by adding different amounts of PVP. The maximum drug-loading of the synthesized SiO₂ NPs is about 30 µg·mg⁻¹, exhibiting excellent pH-responsive drug releasing ability in the simulated physiological environment. Meanwhile, the prepared SiO₂ NPs also harbor well biocompatibility, which are suitable for potential cancer therapy in clinic.

© 2021 The Authors. Published by Atlantis Press B.V.

This is an open access article distributed under the CC BY-NC 4.0 license (<http://creativecommons.org/licenses/by-nc/4.0/>).

1. INTRODUCTION

Tumor is a multiple complex disease, mainly under the influence of external oncogenic factors, abnormal proliferation of cells in local tissues of human body, forming pathological tissue mass [1]. The World Health Organization predicts that in the next 20 years, cancer will become the most important fatal disease, seriously threatening human health and social development [2]. To deal with the huge threat of cancer, researchers all over the world have made great efforts and achieved a series of gratifying results [3]. At present, the main clinical treatment methods of tumor include surgery, radiotherapy and chemotherapy [4]. Comparing with the surgery- and radio-therapy, chemotherapy is one of the main methods of tumor treatment owing to its small invasion, flexible administration and certain curative effect on metastatic tumor [5]. However, the damage of human immunity, cardiovascular disease and liver and kidney function damage are inevitable side effects of chemotherapy.

To improve the process in traditional cancer therapy, the emerged nanosystems for drug delivery are attracting a lot of attentions of researchers due to the properties of easy functionalization, various surface decoration, and good biocompatibility [6]. Based on specific molecules, the surface functionalization of nanomaterials by designed methods provides a broad space for the practical application of nanomaterials [7]. In the field of cancer treatment, nanotechnology has solved many problems for cancer diagnosis and treatment by the interdisciplinary cooperation of chemistry, biology, medicine and imaging [8]. In view of the huge application potential of nanomaterials in the field of cancer treatment,

developing new multifunctional nanomaterials for multimodal therapy is an important and efficient avenue.

Among amounts of alternative materials, Silica Nanoparticles (SiO₂ NPs) possess excellent monodispersity and well biocompatibility which are often designed as nanocarriers to deliver drugs for cancer treatment [9]. In addition, silica can shield the dipole interaction between magnetic particles and prevent particle aggregation [10]. The hydrophilic surface of SiO₂ NPs is easily modified by a variety of silane coupling agents to obtain nanoparticles with different surface functional groups, benefitting for the fabrication of nanosystems to transport drug [11]. Liu et al. [12] prepared a kind of mesoporous SiO₂ NPs conjugated with Polyethyleneimine (PEI), which has targeting integrin $\alpha_v\beta_3$ (RGD) for cancer cells, and successfully targeted the anticancer drug Doxorubicin (DOX). Zhang et al. [13] synthesized an intelligent nanoregulator by coating mesoporous carbon nitride layer on core-shell nitrogen-doped graphene quantum dot @hollow mesoporous silica nanosphere, with decorating by P-PEG-RGD (P-polyethylene glycol-polypeptide with the amino acid sequence of Arg-Gly-Asp) polymer. The obtained nanocomposites achieve a triple-modal ultrasound imaging/infrared thermal imaging/fluorescence imaging (US/IRT/FL) imaging-assisted cooperative photothermal therapy/photodynamic therapy (PTT/PDT) for real-time monitoring of tumor ablation and therapeutic evaluation. Yu et al. developed a kind of nanoplatfrom which can be quickly endocytosis by cells, through using the mesoporous SiO₂ NPs encapsulated with PDS. The nanoplatfrom can transport inhibitory factors and anticancer drugs to tumor cells, realizing the combined therapeutic effect [14]. The unique pore structure of SiO₂ NPs and the hydrophilicity of Si-O bond can effectively adsorb anticancer drugs by physical or hydrogen bonding, keeping them stable in normal physiological

*Corresponding author. Email: zhengyang@fynu.edu.cn

environment (pH = 7.4), which successfully prevents the occurrence of drug burst phenomenon [15]. When SiO₂ NPs is internalized by tumor cells, the lysosome acidic environment (pH = 5.5) can generally accelerate the release of this drug. So that the loaded SiO₂ NPs can accurately release a large number of anticancer drugs in tumor cells, and then kill cancer cells to achieve accurate cancer treatment [16]. Zhang et al. [17] designed a nanoplatform combining by Mn-Cdots, mesoporous silica, and gold cube-in-cubes for a core/shell nanocomposite which could deliver Dox effectively. The obtained nanocomposites perform PDT, PTT, multimodal imaging, and chemotherapy to cancer. Thus, the use of SiO₂ NPs as drug carriers to cure cancer holds huge potential in clinic therapy.

For solving the problems mentioned above, a new method to tailor the nanosize of SiO₂ NPs by adding different amounts of Polyvinyl Pyrrolidone (PVP) is achieved successfully. The synthesized SiO₂ NPs not only possess excellent drug delivering ability for cancer therapy, but also harbor suitable size which is advantageous to the internalization into cancer cells. Meanwhile, the prepared SiO₂ NPs have outstanding biocompatibility, applying in the field of drug delivery competently. Therefore, this work provides a novel avenue for fabrication biocompatible SiO₂ NPs for the potential application in cancer therapy.

2. EXPERIMENTAL SECTION

2.1. Materials and Characterization

Polyvinyl pyrrolidone, ammonia (NH₃·H₂O, 32 wt.%), Tetraethyl Orthosilicate (TEOS), hydrochloric acid (36.0–38.0 wt.%), phosphate buffer saline (PBS) were purchased from Sinopharm Group (China). Dimethyl Sulfoxide (DMSO) was obtained from Sigma-Aldrich Co. LLC (Germany). Propidium Iodide (PI), Hoechst 33342, streptomycin, adriamycin hydrochloride (DOX), trypsin solution (25 wt.%), penicillin, high glucose medium [dulbecco's modified eagle medium (DMEM)], fetal bovine serum and 3-(4,5-dimethylthiazol-2)-2,5-diphenyltetrazolium bromide (MTT) were provided by Shanghai Biotechnology Company (China).

UV-Vis spectra were collected by a U-3900 UV spectrophotometer (Hitachi, Japan) ranging 200–800 nm with deionized (DI) water as the solvent. The morphology and structure of the products were observed on Scanning Electron Microscope (SEM, Sigma 500/VP, the accelerate voltage was 5 kV) and Transmission Electron Microscope (TEM, JEM-100SX, the accelerate voltage was 200 kV). The fluorescent images were captured by an inverted fluorescence microscopy (IX83, Olympus). Fourier Transform Infrared (FT-IR) spectra were obtained on a NEXUS-870 FTIR spectrometer.

2.2. Synthesis of SiO₂ NPs

Typically, a mixture of ethanol and water was prepared at a ratio of 40:10 (v:v), and then 2 ml of ammonia water was added to it. To control the particle size of SiO₂ NPs, 0.5, 1.0 and 1.5 g of surfactant PVP were added to the mixed solution respectively. After ultrasonic dispersion for 30 min until PVP is completely dissolved, stir vigorously for 30 min, and then add 1 ml TEOS to the mixture. After continuous stirring for 24 h, the obtained milky white suspension was centrifuged with 8000 r·min for 10 min. The precipitates were washed with water and ethanol for three times respectively, and then dried at 60°C for 12 h before use.

2.3. Drug Loading and Releasing

2.3.1. DOX loading

20 mg of SiO₂ NPs was added into the 10 ml of DOX solution with a concentration of 100 µg·ml⁻¹. After ultrasonic dispersion for 30 min, the suspension was stirred at room temperature for 24 h. The drug loaded SiO₂ NPs–DOX suspension was centrifuged under 8000 r·min⁻¹ for 10 min, washing by DI water for three times to remove the unloaded drug. Drug loading and encapsulation efficiency were calculated using the following Equation (1):

$$DLE = \frac{m_A - m_s}{m_A} \times 100\% \quad (1)$$

2.3.2. DOX releasing

10 mg of SiO₂ NPs–DOX was added into 10 ml PBS buffer solutions with different pH values (7.4, 6.5 and 5.5) respectively, and oscillated continuously at 37°C. Part of the solution was removed and centrifuged at different time points in 0–72 h. The UV-Vis Spectrum of the supernatant was determined and the release curve was drawn.

2.4. MTT Assay

To determine the apoptosis of SiO₂ NPs–DOX for cancer cells, HepG2 cells were used to evaluate the cytotoxicity by MTT assay. HepG2 cells were seeded on 96-well plates with an initial seeding density of 5 × 10³ cells per well. After 24 h incubation, all wells were washed by PBS for three times. Subsequently, 100 µL of DMEM medium containing 1 mg of SiO₂ NPs–DOX were added into each well respectively. With further co-incubation for different time of 12, 24, 36, and 48 h respectively, the incubated plates were taken out following by washing with PBS for three times. Then, 100 µL of freshly prepared MTT solution (0.5 mg·ml⁻¹) was added into each well for further 4 h incubation. Finally, 200 µL of DMSO was added into wells dissolving the formazan crystals to measure the characteristic absorption at 490 nm by the microplate reader. The control group was incubated without addition of SiO₂ NPs–DOX for the same time. The cell viabilities were calculated by Equation (2):

$$\text{Cell viability} = \frac{OD_{\text{exp}} - OD_{\text{bla}}}{OD_{\text{con}} - OD_{\text{bla}}} \times 100\% \quad (2)$$

where, OD_{bla}, OD_{exp}, and OD_{con} are the optical densities of blank, experimental, and control groups respectively.

2.5. Fluorescent Images

For further investigating the cytotoxicity of SiO₂ NPs–DOX, the relative cell viability was assessed by Hoechst 33342 and PI treated or untreated HepG2 cells. In brief, HepG2 cells were seeded into six-well plates with a density of 5 × 10⁵ each well and incubated at 37°C, 5% CO₂ for 24 h. Sequentially, 2 ml of DMEM suspension containing 20 mg of SiO₂ NPs–DOX were added to each well respectively, followed by the incubation for 12, 24, 36, and 48 h in dark individually. After that, all groups were further washed by PBS buffer (pH 7.4), following with 0.5 ml of Hoechst 33342 (10 µg·ml⁻¹) and 0.5 ml of PI (10 µg·ml⁻¹) adding

to each well staining for 15 min. Finally, the cells were washed by PBS for three times, their fluorescent images were observed and obtained by using an inverted fluorescence microscopy. The control group was treated with the same procedure without adding SiO₂ NPs–DOX.

3. RESULTS AND DISCUSSION

3.1. Characterization of Obtained Samples

To explore the effect of surfactant PVP on the formation of SiO₂ NPs, SiO₂ NPs with different PVP contents (0.5, 1.0 and 1.5 g) were prepared respectively (as shown in Figure 1). The results show that the particle size of SiO₂ NPs decreases with the increase of PVP content, which are about 600 (Figure 1a), 400 (Figure 1b) and 150 nm (Figure 1c), respectively. This is due to the amphiphilic action of PVP to form water in oil (w/o) micro micelles in the mixed solution. The hydrolyzed SiO₂ fragments have hydrophilic surface and are easy to enter the aqueous core of the micelles, and then grow SiO₂ NPs. This monodisperse SiO₂ NPs with a particle size of 150 nm is very suitable for use as a drug carrier in anti-tumor therapy. Therefore, the optimal reaction condition was 1.5 g of PVP. Figure 1d shows the TEM diagram of SiO₂ NPs prepared under the optimal reaction conditions, and the particle size is basically consistent with the SEM of SiO₂ NPs. In addition, the color of SiO₂ NPs is uniform, and there is no obvious hollow structure, so it can be determined that SiO₂ NPs are solid nanoparticles.

For further understanding of the composition of SiO₂ NPs, the prepared SiO₂ NPs were analyzed by FT-IR spectroscopy (Figure 2a). The characteristic peaks at 3420 and 3150 cm⁻¹ correspond to the stretching vibration peaks of –OH, which should be caused by the moisture adsorbed on the surface of the material [18]. The stretching vibration peak of C–H, the stretching vibration peak of C = O and the bending vibration peak of C–H appear at 2980, 1650 and 1400 cm⁻¹ respectively, indicating the existence of PVP in the material [19]. The stretching vibration peaks at 950 and 1050 cm⁻¹ are assigned to Si–OH and Si–O respectively, illustrating the existence of SiO₂ in the material [19]. The above results fully prove that the SiO₂ NPs are nanomaterials composed of SiO₂ and PVP. To determine the content of each component in the product, the samples were also analyzed by thermogravimetry. As shown in Figure 2b, the weight of the product decreases by about 4 wt.% when the temperature changes from 40°C to 100°C, which is caused by the adsorbed water in the sample; in the range of 100–300°C, the weight of the product is reduced by about 6.5 wt.%, which is caused by the volatilization of small molecular organic compounds produced in the preparation process; while at 300–600°C, the weight of the product decreases sharply by about 12.9 wt.%, attributing to PVP in the structure of SiO₂ NPs which is oxidized to CO₂ by air. This result indicates that PVP not only acts as a surfactant and dispersant, but also acts as a structural agent of SiO₂ NPs. Moreover, dynamic light scattering (DLS) analysis was performed as shown in Figure 2c. The average size of SiO₂ NPs in water is around 180 nm, which is slightly larger than the results in Figure 1. This phenomenon may be induced by the solvent effect of H₂O molecules. To investigate the dispersivity of the obtained SiO₂ NPs, Zeta potentials were collected at different pH

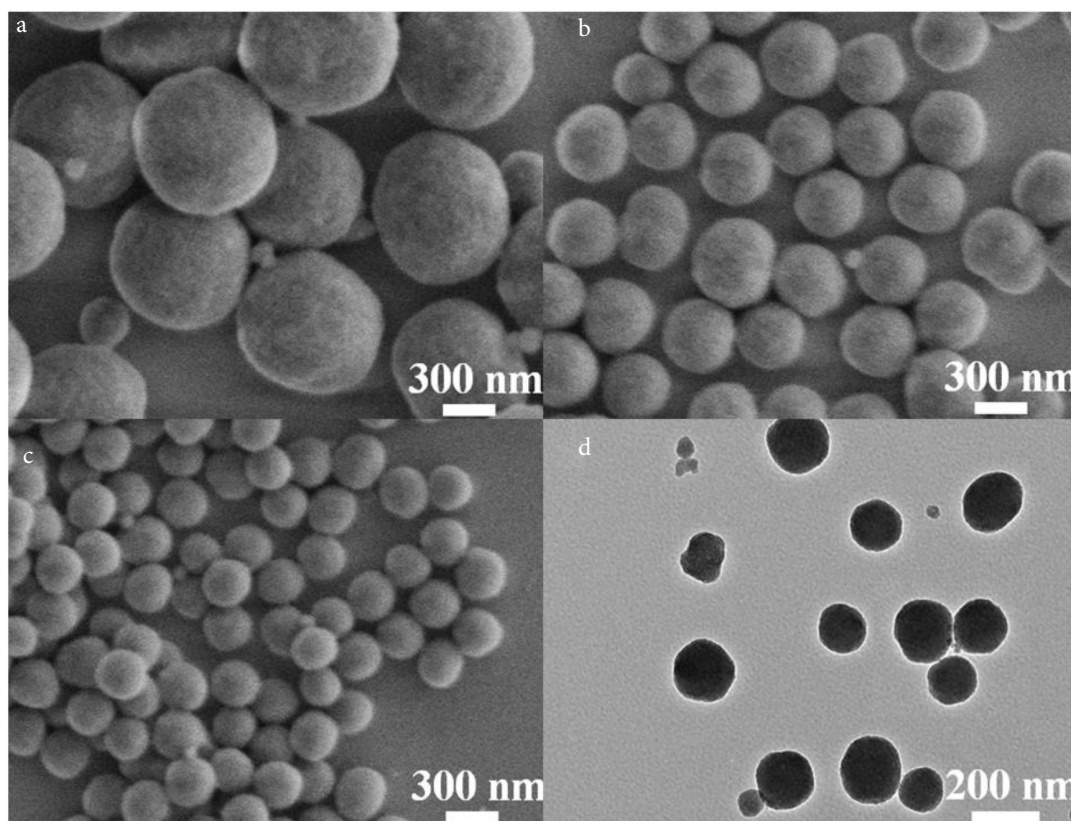


Figure 1 | SEM images of synthesized SiO₂ NPs with the PVP addition of (a) 0.5, (b) 1.0, and (c) 1.5 g, respectively; and (d) TEM image of SiO₂ NP with PVP addition of 1.5 g.

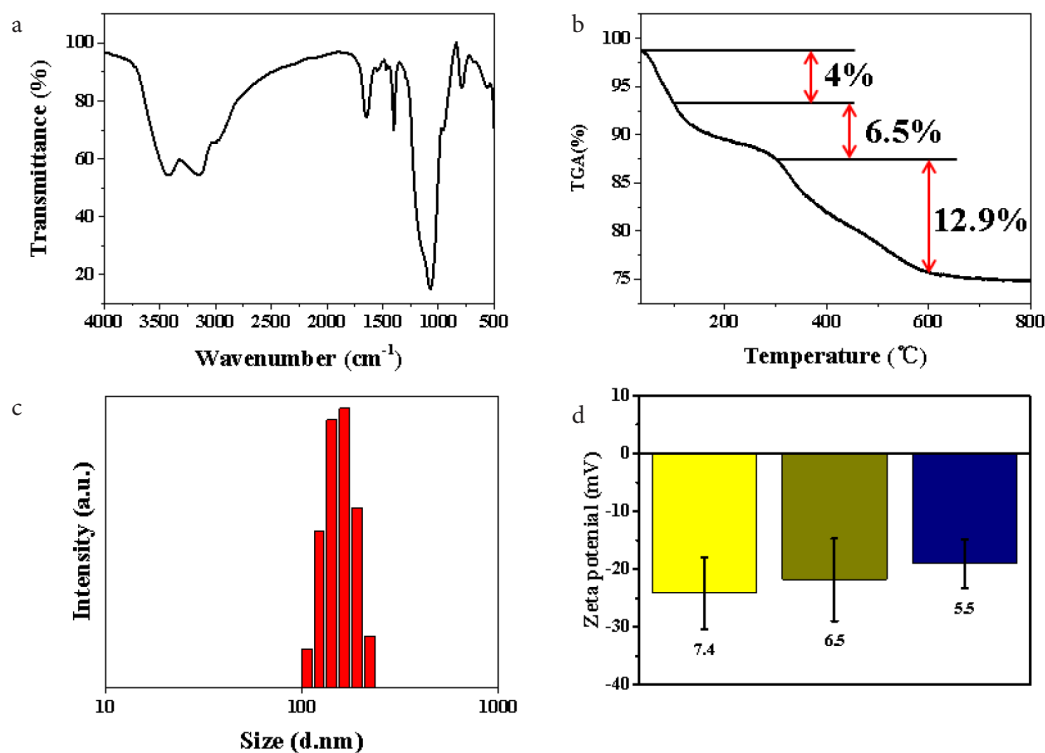


Figure 2 (a) FT-IR spectrum of SiO₂ NPs. (b) Thermogravimetric Analysis (TGA) curve of SiO₂ NPs. (c) DLS analysis of SiO₂ NPs, and (d) Zeta potentials of SiO₂ NPs at different pH values.

values of 7.4, 6.5, and 5.5 to simulate the physiological environment. According to Figure 2d, Zeta potentials of SiO₂ NPs are about −24.0, −22.1, and −20.5 mV at pH values of 7.4, 6.5, and 5.5 respectively, which demonstrating the well dispersivity of SiO₂ NPs under physiological conditions. These proofs confirm that the prepared SiO₂ NPs are suitable nanocarriers to deliver DOX in anti-cancer application.

To investigate the DOX loading performance of the prepared SiO₂ NPs, the UV-Vis spectra of DOX solution before and after loading with SiO₂ NPs were plotted respectively (Figure 3a). The black curve is the UV-Vis spectrum of DOX solution. It can be seen that there is a characteristic absorption peak of DOX at 248 nm, which is caused by π - π^* transition in DOX molecule, and the secondary absorption peak at 490 nm is caused by n - π^* transition [20]. According to the red curve in the figure, the same secondary absorption peak as DOX solution appears at 490 nm, indicating that SiO₂ NPs has successfully loaded DOX. The loading amount of DOX in SiO₂ NPs-DOX complex is about 30 $\mu\text{g}\cdot\text{mg}^{-1}$, which indicates that the prepared SiO₂ NPs are useful drug carrier with large capacity. Figure 3b shows the drug release curve of SiO₂ NPs-DOX complex in PBS with different pH values. The pH values of 7.4, 6.5 and 5.5 simulated the pH conditions of normal physiological environment, tumor local microenvironment and cytolysin *in vivo* environment respectively [20]. The result shows that the release rate of DOX is very slow in the SiO₂ NPs-DOX dispersion with pH = 7.4. After 24 h, the release rate of DOX is only about 8% of the total load, while the total release of DOX is about 10% after 48 h. At pH = 6.5, the release rate of DOX increased obviously, about 27% of the total load was released after 24 h, and the total release of DOX reached about 38% after 48 h. These results indicate that SiO₂ NPs-DOX has a typical pH response, which can induce the release of drugs in the simulated local microenvironment of tumor, so as to transport the drugs to the tumor site and achieve

precise chemotherapy effect. In addition, under the condition of pH = 5.5, the release rate of DOX is very fast, which reaches about 60% of the total load after 24 h, and almost completely releases the loaded DOX at about 48 h. The experimental results fully show that the prepared SiO₂ NPs-DOX complex can release the loaded chemotherapeutic drugs completely after entering the lysosomal environment, thus promoting the rapid increase of drug concentration in tumor cells in a short time, and then lead to the death of tumor cells. Therefore, the prepared SiO₂ NPs are excellent drug carriers with high drug loading, and can respond to the pH of tumor micro-environment to realize the drug release process of pH control.

According to the MTT test results of HepG2 cells co-cultured with different concentrations of SiO₂ NPs for 48 h in Figure 4a, the survival rates of HepG2 cells at all concentrations were more than 90%. The results show that the prepared SiO₂ NPs possess good biocompatibility, without affecting the normal growth of HepG2 cells, which are suitable to be used as drug carriers in the field of tumor therapy [21]. For further study of the therapeutic effect of SiO₂ NPs-DOX complex to HepG2 cells, MTT tests were performed at different time points after co-culture of SiO₂ NPs-DOX complex with HepG2 cells (Figure 4b). With the increase of culture time (12, 24, 36 and 48 h), the survival rate of HepG2 cells decreased to about 60%, 51%, 29% and 18%, respectively. The main reason for this result is that HepG2 cells phagocytized a large number of SiO₂ NPs-DOX complexes, and over time, SiO₂ NPs-DOX complexes released a large number of DOX in the lysosome, which led to a wide range of HepG2 cell death. Therefore, the prepared SiO₂ NPs are valuable drug carriers, which can release the drug with pH response in tumor cells, achieving the precise treatment of tumor cells.

Figure 5 showed the fluorescence microscopy images of composites incubated with HepG2 cells and dyed by Hoechst 33342 and PI.

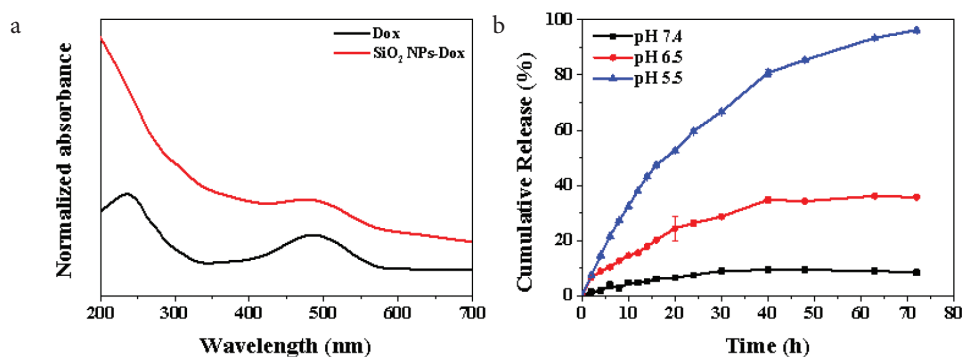


Figure 3 | (a) UV-Vis spectra of DOX (black) and SiO₂ NPs-DOX (red) and (b) release curve of DOX at different pH from SiO₂ NPs-DOX.

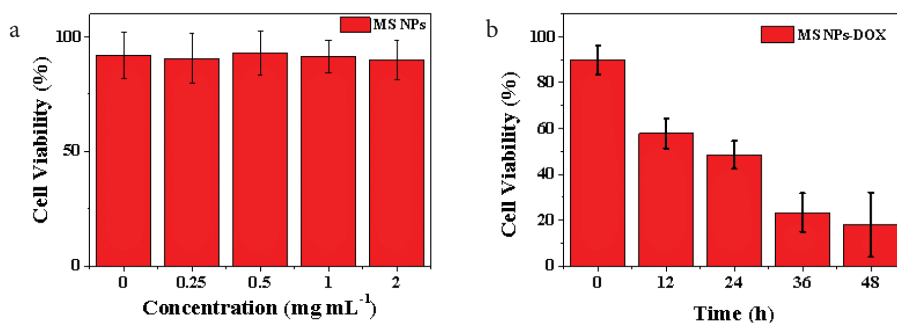


Figure 4 | (a) The cell viabilities of HepG2 cells co-incubated with different concentrations of SiO₂ NPs (0.25, 0.5, 1, and 2 mg·mL⁻¹) for 48 h and (b) *in vitro* therapy effects of SiO₂ NPs-DOX composites (0.5 mg·mL⁻¹) against HepG2 cells at different time points (0–48 h).

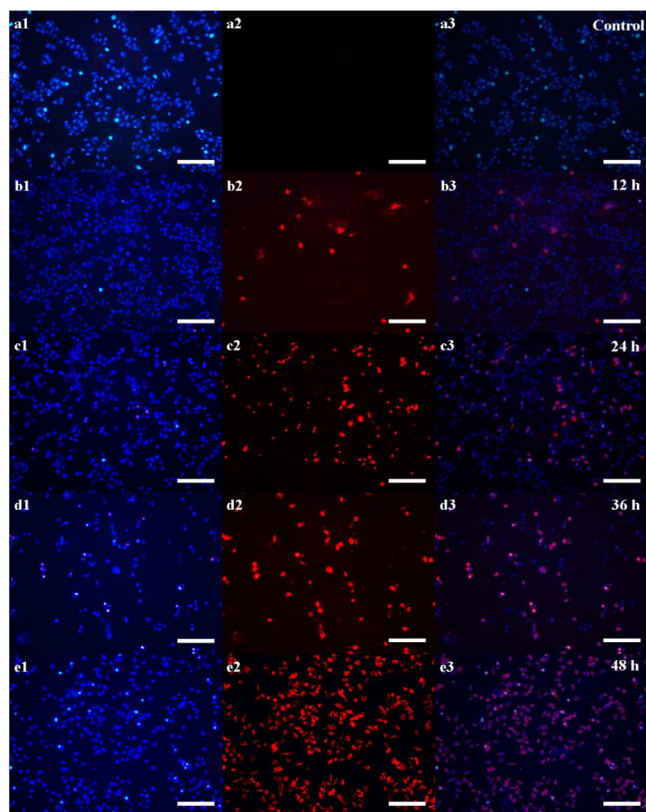


Figure 5 | Fluorescence images of (a) control group, and (b–e) SiO₂ NPs-DOX treated groups incubating after different time points of 12, 24, 36, and 48 h respectively, which blue and red fluorescence are stained by Hoechst 33342 and PI individually (Scale bar: 200 μm).

In Figure 5a2, the image of control group displays ignorable red fluorescence, indicating all cells grow well under this condition [22]. This result demonstrates the synthesized SiO₂ NPs harbor outstanding biocompatibility, benefitting for biomedical application. Moreover, a few cells died after 12 h co-incubation with SiO₂ NPs-DOX, showing faint red fluorescence in Figure 5b2. Following with the increase of the co-incubation time to 24 h, obvious red fluorescence can be found in Figure 5c2, which indicates more cells are killed by the released DOX from SiO₂ NPs-DOX. When the co-incubation time extends to 36 h, Figure 5d2 displays intense red fluorescence demonstrates large amounts of DOX are released by SiO₂ NPs-DOX inducing the extensive apoptosis. The most important evidence coming from Figure 5e2, nearly all cells are killed after 48 h co-incubation with the enhanced red fluorescence, illustrating that the loaded DOX in SiO₂ NPs-DOX is released totally. All results above prove adequately that the synthesized SiO₂ NPs are excellent carriers for drug delivery, achieving the pH-responsive drug release for cancer treatment.

4. CONCLUSION

A new method for fabricating PVP-induced SiO₂ NPs was achieved successfully. The prepared SiO₂ NPs with size of ca. 150 nm were tailored by the addition of different amounts of PVP. The synthesized SiO₂ NPs possess excellent drug delivering ability for DOX, which is up to about 30 μg·mg⁻¹. Moreover, the SiO₂ NPs-DOX also exhibit outstanding pH-responsive drug releasing property in the simulated physiological environment. The drug loaded SiO₂ NPs-DOX could induce obvious apoptosis of HepG2 cells, harboring huge potential in the anticancer application for clinic. Our

work provides a useful way to prepare novel nanocarriers for drug delivery to cure cancer.

CONFLICTS OF INTEREST

The authors declare they have no conflicts of interest.

AUTHORS' CONTRIBUTION

WY performed all experiments and analyzed the data. ZY checked the results and wrote the paper.

ACKNOWLEDGMENTS

This work is supported by the Natural Science Foundation of Anhui Province (No. 1908085QE224), and Talent Project of Fuyang Normal University (No. 2018kyqd0034). Authors also want to thank the National Students Research Training Program (No. 202010371017) and Students Research Training Program of Anhui Province (No. S201910371023).

REFERENCES

- [1] Mohammad HP, Barbash O, Creasy CL. Targeting epigenetic modifications in cancer therapy: erasing the roadmap to cancer. *Nat Med* 2019;25:403–18.
- [2] Bor G, Mat Azmi ID, Yaghmur A. Nanomedicines for cancer therapy: current status, challenges and future prospects. *Ther Deliv* 2019;10:113–32.
- [3] Sandra F, Khaliq NU, Sunna A, Care A. Developing protein-based nanoparticles as versatile delivery systems for cancer therapy and imaging. *Nanomaterials (Basel)* 2019;9:1329.
- [4] van der Meel R, Sulheim E, Shi Y, Kiessling F, Mulder WJM, Lammers T. Smart cancer nanomedicine. *Nat Nanotechnol* 2019;14:1007–17.
- [5] Hinge N, Pandey MM, Singhvi G, Gupta G, Mehta M, Satija S, et al. Nanomedicine advances in cancer therapy. In: Lisa C. du Toit, Pradeep Kumar, Yahya E. Choonara, Viness Pillay, editors. *Advanced 3D-printed systems and nanosystems for drug delivery and tissue engineering*. Amsterdam: Elsevier; 2020, pp. 219–53.
- [6] Zhang X. Clinical applications of tumor-targeted systems. In: Huang R, Wang Y, editors. *New nanomaterials and techniques for tumor-targeted systems*. Singapore: Springer; 2020, pp. 437–56.
- [7] Lu ZR, Qiao P. Drug delivery in cancer therapy, quo vadis? *Mol Pharm* 2018;15:3603–16.
- [8] Kalaydina RV, Bajwa K, Qorri B, Decarlo A, Szewczuk MR. Recent advances in “smart” delivery systems for extended drug release in cancer therapy. *Int J Nanomedicine* 2018;13:4727–45.
- [9] Shen D, Yang J, Li X, Zhou L, Zhang R, Li W, et al. Biphasic stratification approach to three-dimensional dendritic biodegradable mesoporous silica nanospheres. *Nano Lett* 2014;14:923–32.
- [10] Pellen-Mussi P, Tricot-Doleux S, Neaime C, Nerambourg N, Cabello-Hurtado F, Cordier S, et al. Evaluation of functional SiO₂ nanoparticles toxicity by a 3D culture model. *J Nanosci Nanotechnol* 2018;18:3148–57.
- [11] Huang L, Liu J, Gao F, Cheng Q, Lu B, Zheng H, et al. A dual-responsive, hyaluronic acid targeted drug delivery system based on hollow mesoporous silica nanoparticles for cancer therapy. *J Mater Chem B* 2018;6:4618–29.
- [12] Liu Z, Chen W, Li Y, Xu Q. Integrin $\alpha_v\beta_3$ -targeted C-dot nanocomposites as multifunctional agents for cell targeting and photoacoustic imaging of superficial malignant tumors. *Anal Chem* 2016;88:11955–62.
- [13] Zhang X, Ong'achwa Machuki J, Pan W, Cai W, Xi Z, Shen F, et al. Carbon nitride hollow theranostic nanoregulators executing laser-activatable water splitting for enhanced ultrasound/fluorescence imaging and cooperative phototherapy. *ACS Nano* 2020;14:4045–60.
- [14] Yu C, Qian L, Ge J, Fu J, Yuan P, Yao SCL, et al. Cell-penetrating poly(disulfide) assisted intracellular delivery of mesoporous silica nanoparticles for inhibition of miR-21 function and detection of subsequent therapeutic effects. *Angewandte Chemie* 2016;55:9272–6.
- [15] Mo J, He L, Ma B, Chen T. Tailoring particle size of mesoporous silica nanosystem to antagonize glioblastoma and overcome blood–brain barrier. *ACS Appl Mater Interfaces* 2016;8:6811–25.
- [16] Zhao W, Wang K, Wei Y, Ma Y, Liu L, Huang X. Laccase biosensor based on phytic acid modification of nanostructured SiO₂ surface for sensitive detection of dopamine. *Langmuir* 2014;30:11131–7.
- [17] Zhang X, Xi Z, Machuki JO, Luo J, Yang D, Li J, et al. Gold cube-in-cube based oxygen nanogenerator: a theranostic nanoplatfor for modulating tumor microenvironment for precise chemophototherapy and multimodal imaging. *ACS Nano* 2019;13:5306–25.
- [18] Li P, Liu L, Lu Q, Yang S, Yang L, Cheng Y, et al. Ultrasmall MoS₂ nanodots-doped biodegradable SiO₂ nanoparticles for clearable FL/CT/MSOT imaging-guided PTT/PDT combination tumor therapy. *ACS Appl Mater Interfaces* 2019;11:5771–81.
- [19] Zhou S, Ding C, Wang Y, Jiang W, Fu J. Supramolecular valves functionalized rattle-structured UCNPs@hm-SiO₂ nanoparticles with controlled drug release triggered by quintuple stimuli and dual-modality imaging functions: a potential theranostic nanomedicine. *ACS Biomater Sci Eng* 2019;5:6022–35.
- [20] Wang TT, Wei QC, Zhang ZT, Lin MT, Chen JJ, Zhou Y, et al. AIE/FRET-based versatile PEG-Pep-TPE/DOX nanoparticles for cancer therapy and real-time drug release monitoring. *Biomater Sci* 2020;8:118–24.
- [21] Xia Y, Xu T, Wang C, Li Y, Lin Z, Zhao M, et al. Novel functionalized nanoparticles for tumor-targeting co-delivery of doxorubicin and siRNA to enhance cancer therapy. *Int J Nanomedicine* 2017;13:143–59.
- [22] Zheng Y, You X, Chen L, Huang J, Wang L, Wu J, et al. Biotherapeutic nanoparticles of poly(ferulic acid) delivering doxorubicin for cancer therapy. *J Biomed Nanotechnol* 2019;15:1734–43.